THE JOURNAL OF BIOLOGICAL CHEMISTRY VOL. 288, NO. 17, pp. 12232–12243, April 26, 2013
Published in the U.S.A.

PDZ-RhoGEF and LARG Are Essential for Embryonic Development and Provide a Link between Thrombin and LPA Receptors and Rho Activation*[S]

Received for publication, October 16, 2012, and in revised form, March 4, 2013 Published, JBC Papers in Press, March 6, 2013, DOI 10.1074/jbc.M112.428599

Constantinos M. Mikelis[‡], Todd R. Palmby[‡1], May Simaan[‡], Wenling Li[§], Roman Szabo[‡], Ruth Lyons[‡2], Daniel Martin[‡], Hiroshi Yagi[‡3], Shigetomo Fukuhara[‡4], Hiroki Chikumi[‡5], Rebeca Galisteo[‡], Yoh-suke Mukouyama[§], Thomas H. Bugge[‡], and J. Silvio Gutkind[‡6]

From the [‡]Oral and Pharyngeal Cancer Branch, NIDCR, and the [§]Laboratory of Stem Cell and Neuro-Vascular Biology, Genetics and Developmental Biology Center, NHLBI, National Institutes of Health, Bethesda, Maryland 20892

Background: Many Rho GEFs have been proposed to link GPCRs to Rho activation.
Results: PDZ-RhoGEF and LARG double deficiency leads to embryonic lethality and, along with p115 RhoGEF, are required for thrombin-induced cell migration, proliferation, and RhoA activation.
Conclusion: PDZ-RhoGEF, LARG, and p115 RhoGEF mediate $G\alpha_{12/13}$ signaling to RhoA.
Significance: These findings identify novel targets for pharmacological intervention in diseases involving aberrant GPCR signaling.

G protein-coupled receptors (GPCRs) linked to both members of the $G\alpha_{12}$ family of heterotrimeric G proteins α subunits, $G\alpha_{12}$ and $G\alpha_{13}$, regulate the activation of Rho GTPases, thereby contributing to many key biological processes. Multiple Rho GEFs have been proposed to link $G\alpha_{12/13}$ GPCRs to Rho activation, including PDZ-RhoGEF (PRG), leukemia-associated Rho GEF (LARG), p115-RhoGEF (p115), lymphoid blast crisis (Lbc), and Dbl. PRG, LARG, and p115 share the presence of a regulator of G protein signaling homology (RGS) domain. There is limited information on the biological roles of this RGS-containing family of RhoGEFs *in vivo*. p115-deficient mice are viable with some defects in the immune system and gastrointestinal motor dysfunctions, whereas in an initial study we showed that mice deficient for Larg are viable and resistant to salt-induced hypertension. Here, we generated knock-out mice for Prg and observed that these mice do not display any overt phenotype. However, deficiency in Prg and Larg leads to complex developmental defects and early embryonic lethality. Signaling from $G\alpha_{11/q}$-linked GPCRs to Rho was not impaired in mouse embryonic fibroblasts defective in all three RGS-containing RhoGEFs. However, a combined lack of Prg, Larg, and p115 expression abolished signaling through $G\alpha_{12/13}$ to Rho and thrombin-induced cell proliferation, directional migration, and nuclear signaling through JNK and p38. These findings provide evidence of an essential role for the RGS-containing RhoGEF family in signaling to Rho by $G\alpha_{12/13}$-coupled GPCRs, which may likely play a critical role during embryonic development.

The family of mammalian Rho GTPases represents a branch within the Ras superfamily of small GTP-binding proteins, which plays a key role in multiple biological functions, ranging from morphogenesis, polarity, migration, neural development, cellular division and adhesion, vesicle transport, microtubule dynamics, and cell cycle progression to gene expression (1–3). Rho GTPases are activated by a variety of extracellular stimuli acting on cell surface receptors such as tyrosine kinase receptors, G protein-coupled receptors (GPCRs),[7] and cell-cell and cell-matrix adhesion molecules, such as cadherins and integrins (4). The most highly conserved Rho GTPases are Rho, Rac, and Cdc42, which act as molecular switches between an active GTP-bound form and an inactive GDP-bound form (1). The cycling between these two stages is regulated by three classes of regulatory proteins, 1) the guanine nucleotide-exchange factors (GEFs) that catalyze the transition from an inactive, GDP-bound to an active, GTP-bound state; 2) the GTPase-activating proteins that accelerate GTP hydrolysis and hence promote the termination of Rho GTPase signaling; and 3) the guanine nucleotide dissociation inhibitors that sequester GTPases in the cytosol in a GDP-bound state (2, 5).

Most cell surface receptors control the activity of Rho GTPases by promoting the activation of a large variety of GEFs

* This work was supported, in whole or in part, by National Institutes of Health Grant Z01DE00551 and the Intramural Research Program of the NIDCR, National Institutes of Health.
[S] This article contains supplemental Movies S1–S5.
[1] Present address: Office of Hematology and Oncology Products, Office of New Drugs, Center for Drug Evaluation and Research, United States Food and Drug Administration, Silver Spring, MD 20993.
[2] Present address: Kinghorn Cancer Centre, Garvan Inst. of Medical Research, 370 Victoria St., Darlinghurst, Sydney, NSW 2010, Australia.
[3] Present address: Dept. of Obstetrics and Gynecology, Graduate School of Medical Sciences, Kyushu University, Fukuoka, Japan.
[4] Present address: Dept. of Cell Biology, National Cerebral and Cardiovascular Center Research Institute, 5-7-1 Fujishirodai, Suita, Osaka 565-8565, Japan.
[5] Present address: Div. of Medical Oncology and Molecular Respirology, Dept. of Multidisciplinary Internal Medicine, Faculty of Medicine, Tottori University, 36-1 Nishi-cho, Yonago-shi, Tottori-ken 683-8504, Japan.
[6] To whom correspondence should be addressed: 30 Convent Dr., Bldg. 30, Rm. 211, NIDCR/NIH, Bethesda, MD 20892-4340. Tel.: 301-496-6259; Fax: 301-402-0823; E-mail: sg39v@nih.gov.

[7] The abbreviations used are: GPCR, G protein-coupled receptor; PRG, PDZ-RhoGEF; LARG, leukemia-associated Rho GEF; p115, p115-RhoGEF; RGS, regulator of G protein signaling homology; GEF, guanine nucleotide-exchange factor; Lbc, lymphoid blast crisis; MEF, mouse embryonic fibroblast; E, embryonic day.

(5). Among them, the Dbl family of Rho GEFs is the largest, with 69 homologs in humans (5). This family is characterized by the Dbl homology domain, which is a ~200-amino acid helical domain, followed by a pleckstrin homology domain. The Dbl homology domain is responsible for the nucleotide exchange activity toward GTPases of the Rho family, and the pleckstrin homology domain is essential for full GEF activity and also binds to other signaling molecules, including phospholipids and intracellular proteins and contributes to the proper localization of the Dbl homology domain (5). Other important structural features of Rho GEFs include regulator of G protein signaling homology (RGS homology) and PDZ domains and coiled-coil oligomerization, proline-rich, acidic autoinhibitory, and actin-binding motifs, many of which contribute to the regulation of the Dbl homology-pleckstrin homology GEF function (6).

GPCRs initiate signaling at the level of the plasma membrane, thereby regulating their membrane, cytoplasmic, and nuclear targets by interacting with heterotrimeric G proteins composed by α, β, and γ subunits. The G protein α subunits are divided into four subfamilies: $G\alpha_i$, $G\alpha_s$, $G\alpha_q$, and $G\alpha_{12}$. Members of the $G\alpha_q$ and $G\alpha_{12}$ subfamilies have been shown to regulate the activation of several small GTPases of the Ras and Rho families (reviewed in Ref. 7). In this regard, multiple Rho GEFs that have been proposed to link $G_{12/13}$-coupled GPCRs to Rho activation, including PDZ-RhoGEF (PRG), leukemia-associated Rho GEF (LARG), p115-RhoGEF (p115), and lymphoid blast crisis (Lbc), its longer transcript fused to an AKAP (A kinase anchor protein), AKAP-Lbc (8, 9), proto-Dbl (10, 11), and Lfc (12). Among them, PRG, LARG, and p115 share the presence of a RGS homology domain, which is responsible for their interaction with $G\alpha_{12}$ and its family member, $G\alpha_{13}$ (6, 8, 13). Lbc has a C-terminal region that shares low amino acid identity to the consensus RGS domain and is called "RGS-like" (14). PRG and LARG also contain a PDZ domain in their N terminus, which is responsible for protein-protein interactions, binding the C termini of proteins harboring PDZ-binding motifs (8, 15). For example, both PRG and LARG can associate through the PDZ-binding region with Plexin B (16, 17), with LPA-1 and -2 receptors (18), and the insulin-like growth factor-1 receptor (19). The C-terminal region of PRG and LARG also seems to have important functions, because it can be tyrosine-phosphorylated by focal adhesion kinase (20) and mediates the formation of homo- and hetero-oligomers (21). Some studies have also suggested the functional interaction of LARG with $G\alpha_q$ (22).

There is still limited information of the function of PRG, LARG, and p115 *in vivo*. p115-deficient mice are viable with defects in lymphocyte motility and immune responses and motor dysfunction in the gastrointestinal tract (23). In initial studies, we have observed that mice deficient for Larg are also viable and are resistant to salt-induced hypertension (24). The consequences of Prg deficiency are largely unknown. Here, we generated knock-out mice for Prg and observed no major anatomical defects. Given the structural similarities between Prg and Larg, we next investigated the consequence of the double deficiency in both GEFs. Interestingly, mice deficient in both Prg and Larg display complex developmental defects and die during early stages of embryogenesis. Furthermore, isolation of mouse embryonic fibroblasts (MEFs) from wild type and double-deficient mice, combined with the efficient knockdown of p115, enabled us to elucidate the role of these GEFs on Rho activation. Whereas cells defective for all three RGS-containing RhoGEFs did not display compromised $G_{11/q}$ signaling to Rho, signaling through $G_{12/13}$ to Rho was abolished in cells lacking RGS-containing RhoGEF. In these cells, thrombin was not able to induce cell proliferation and directional migration and failed to initiate nuclear signaling through JNK and p38. These findings provide evidence of an essential role for the RGS-containing RhoGEF family in signaling to Rho by $G_{12/13}$-coupled GPCRs, which may likely play a critical role during embryonic development.

EXPERIMENTAL PROCEDURES

Targeting Vector Construction—Targeted disruption of the murine *Arhgef11* (referred herein as *PDZ-RhoGEF*, or *Prg*) (see Fig. 1*A*) and *Arhgef12* (referred herein as *Larg*) (see Fig. 1*B*) genes. The genomic clone used for gene targeting contained the second and third exons of the *Prg* gene (A) and the first exon of the *Larg* gene (B). To generate a null mutation, we replaced a 2-kb BsaI to EcoRI fragment containing the second and third exon of *Prg* gene (A) and a 1.6-kb BamHI to HindIII fragment containing the first exon of *Larg* gene (B) by the neomycin resistance (*Neo*) cassette. Gene targeting in mouse embryonic stem cell line was done as described (25). Correctly targeted embryonic stem cell clones were injected into C57BL/6 blastocysts, and chimeras were bred with C57BL/6 mice to generate heterozygous animals (25). Targeting of *Prg* (A) and *Larg* (B) genes and germ line transmission of the targeted alleles were confirmed by Southern blotting. Genotyping of mice was performed by PCR amplification of DNA from ear or tail biopsies with the primers for *Prg* (*Prg* forward, 5′-CTGGTGAAATGTGGTGTGTTGAAGG-3′; *Prg* WT reverse, 5′-GATGGCACCTGGACATTTAGTACTAAG-3′; *Prg* knock-out reverse, 5′-GCTAAAGCGCATGCTCCAGACTGC-3′) and *Larg* (*Larg* forward, 5′-GTCGCTTGATGTTTACAGGCAGAAT-3′; *Larg* WT reverse, 5′-GGCCAGAAGAGGCTGTGGAGAAAG-3′; *Larg* knock-out reverse, 5′-GCTAAAGCGCATGCTCCAGACTGC-3′) primers.

Cell Lines, Culture Procedures, DNAs, and Reagents—HEK-293T cells were cultured in DMEM containing 10% FBS and 1× antibiotic/antimycotic solution (Sigma-Aldrich). MEFs were isolated from E8.5 wild type and Prg and Larg double-deficient embryos as described previously (26) and were cultured in DMEM-containing 10% FBS and antibiotic/antimycotic solution. Control shRNA and shRNAs for murine p115 Rho GEF (NM_001130150) (catalog no. RMM3981-98070064 and RMM3981-98069990) in pLKO1 lentiviral vectors were obtained from Open Biosystems (Lafayette, CO). Lentiviral stocks were prepared with HEK-293T cells as the packaging cells, as described previously (27). After infection, the mouse embryonic fibroblasts were selected for 20 days in DMEM. 10% FBS with 1 μg/ml puromycin (Invivogen, San Diego, CA). Thrombin and LPA were purchased from Sigma-Aldrich (catalog nos. T4648 and L7260, respectively).

Extraction of Embryonic and Perinatal Tissues—Breeding females were checked for vaginal plugs each morning, and the day on which the plug was found was defined as the first day of pregnancy (E0.5). The pregnant females were euthanized in the mid-day at designated time points by CO_2 inhalation. The embryos were extracted by Caesarian section, and the individual embryos, yolk sacs, and placentae were dissected and processed as described below. The visceral yolk sacs of individual embryos were washed twice in phosphate-buffered saline, subjected to genomic DNA extraction, and genotyped by PCR (primer sequences shown above).

Histopathological Analysis—For histological analysis of Prg- and Larg-deficient embryos, the embryos and extraembryonic tissues were fixed for 18–20 h in 4% paraformaldehyde in PBS, processed into paraffin, sectioned and stained with hematoxylin and eosin, or used for immunohistochemistry as described below.

Immunohistochemistry—Unstained 5-μm paraffin sections were dewaxed in Safeclear II (Fisher) hydrated through graded alcohols and distilled water and washed three times with PBS. The antigens were retrieved by incubation for 10 min at 37 °C with 10 μg/ml proteinase K (Fermentas, Hanover, MD) for HAI-1 staining or by incubation for 20 min at 100 °C in 0.01 M sodium citrate buffer, pH 6.0, for all other antigens. The sections were blocked with 2% bovine serum albumin in PBS and incubated overnight at 4 °C with 1:100 dilution of rat anti-mouse CD34 (BD Biosciences) or goat anti-mouse HAI-1 (R&D Systems, Minneapolis, MN) primary antibodies. Bound antibodies were visualized using 1:400 dilution of biotin-conjugated anti-mouse, -rabbit, -sheep, or -goat secondary antibodies (Vector Laboratories, Burlingame, CA) and a Vectastain ABC kit (Vector Laboratories) using 3,3′-diaminobenzidine as the substrate (Sigma-Aldrich). Substrate development was stopped in distilled water. The slides were thoroughly washed, counterstained with Mayer's hematoxylin, dehydrated, and mounted. Immunohistochemically stained whole slide images were acquired with an Aperio CS Scanscope (Aperio, Vista, CA) with a 40× magnification, and slides were stained with CD34 were quantified using the IHC Microvessels Algorithm (Aperio, Vista, CA).

Whole Mount Immunohistochemistry—Mouse embryos or yolk sacs were dissected at E10.5, fixed in 4% paraformaldehyde/PBS at 4 °C for 1 h, and rinsed three times with PBS. Immunostaining was performed using anti-PECAM-1 primary antibody (rat monoclonal antibody, clone MEC13.3 (BD Pharmingen), 1:200, overnight at 4 °C) followed by HRP-conjugated secondary antibody (Jackson; 1:200, overnight at 4 °C). All of the images were captured using a Q-image camera (Leica).

Immunoblot Analysis—The cells were lysed on ice in lysis buffer (50 mM Tris-HCl, 150 mM NaCl, 1% Nonidet P-40) supplemented with protease inhibitors (0.5 mM phenylmethylsulfonyl fluoride, 10 μg/ml aprotinin, and 10 μg/ml leupeptin). Equal amounts of proteins were subjected to SDS-PAGE and transferred onto an Immobilon P, polyvinylidene difluoride membrane (Millipore, Billerica, MA). The membranes were then incubated with the appropriate antibodies: PDZ-RhoGEF (sc-46232 1:500), LARG (sc-25638 1:500), p115 (sc-20804 1:500) (all from Santa Cruz Biotechnology, Santa Cruz, CA), a-RhoA (catalog no. 2117 1:2000), pERK (catalog no. 4370 1:3000), ERK (catalog no. 9102 1:5000), p-p38 (catalog no. 4511 1:3000), p38 (catalog no. 9212 1:3000), pJNK (catalog no. 4668 1:3000), JNK (catalog no. 9258 1:3000), β-actin (catalog no. 4967 1:5000), and tubulin (catalog no. 3873 1:5000) (all from Cell Signaling Technology, Beverly, MA). The antigens were visualized using the Immobilon Western Chemiluminescent HRP substrate (Millipore).

Rho GTPase Pulldown Assay—Rho activation in cultured cells was assessed by a modification of a method described elsewhere (21). Briefly, after serum starvation for 3 h, the cells were treated as indicated and lysed on ice in a buffer containing 20 mM Hepes, pH 7.4, 0.1 M NaCl, 1% Triton X-100, 10 mM EGTA, 40 mM β-glycerophosphate, 20 mM $MgCl_2$, 1 mM Na_3VO_4, 1 mM dithiothreitol, 10 μg/ml aprotinin, 10 μg/ml leupeptin, and 1 mM phenylmethylsulfonyl fluoride. The lysates were incubated with GST-rhotekin-Rho binding domain previously bound to glutathione-Sepharose beads (Amersham Biosciences) and washed three times with lysis buffer. Associated GTP-bound forms of Rho were released with SDS/PAGE loading buffer and analyzed by Western blot analysis using a monoclonal antibody against RhoA, as described above.

DNA Synthesis (EdU Incorporation) Assay—To visualize individual cells synthesizing DNA, we used the Click-It kit (Invitrogen) according to the manufacturer's instructions. Briefly, subconfluent cells were grown on fibronectin-coated coverslips (Invitrogen), serum-starved, and induced using the appropriate mitogen for 16 h. Then EdU (10 μM) was added for 4 h, and cells were fixed in a 4% paraformaldehyde/PBS solution (Electron Microscopy Sciences, Hatfield, PA). Samples were mounted in Vectashield containing DAPI mounting medium (Vector Laboratories) and visualized under Axio Imager Z1 microscope equipped with ApoTome system controlled by AxioVision software (Carl Zeiss, Thornwood, NY).

Cell Migration Assay—Migration assays were performed as described previously (28) using a 48-well Boyden chamber with an 8-μm pore size polyvinyl pyrrolidone-free polycarbonate membrane (NeuroProbe) coated with fibronectin. Mouse embryonic fibroblasts from WT mice infected with the vector (pLKO1) or double-deficient for Prg and Larg mice infected with shRNA for p115 were added to the upper chamber, and thrombin (0.1 unit/ml) was added to the lower chamber in serum-free DMEM. After incubation for 6 h at 37 °C, the cells on the upper surface of the membrane were removed, and the cells on the lower surface were fixed and stained. Images of the entire lower surface of the membranes were taken, and the number of migrated cells was counted (four wells per condition).

Wound Healing Assay—Cell motility was measured by both Boyden chamber assay and wound healing migration assay. Mouse embryonic fibroblasts from WT mice infected with the vector (pLKO1) and double knock-out (−/−) for *Prg* and *Larg* mice infected with shRNA lentiviruses for p115 were grown to a confluent monolayer inside Culture-inserts (Ibidi, Verona, WI; catalog no. 80241), according to manufacturer's instructions. After wounding, loose cells or cell debris were removed

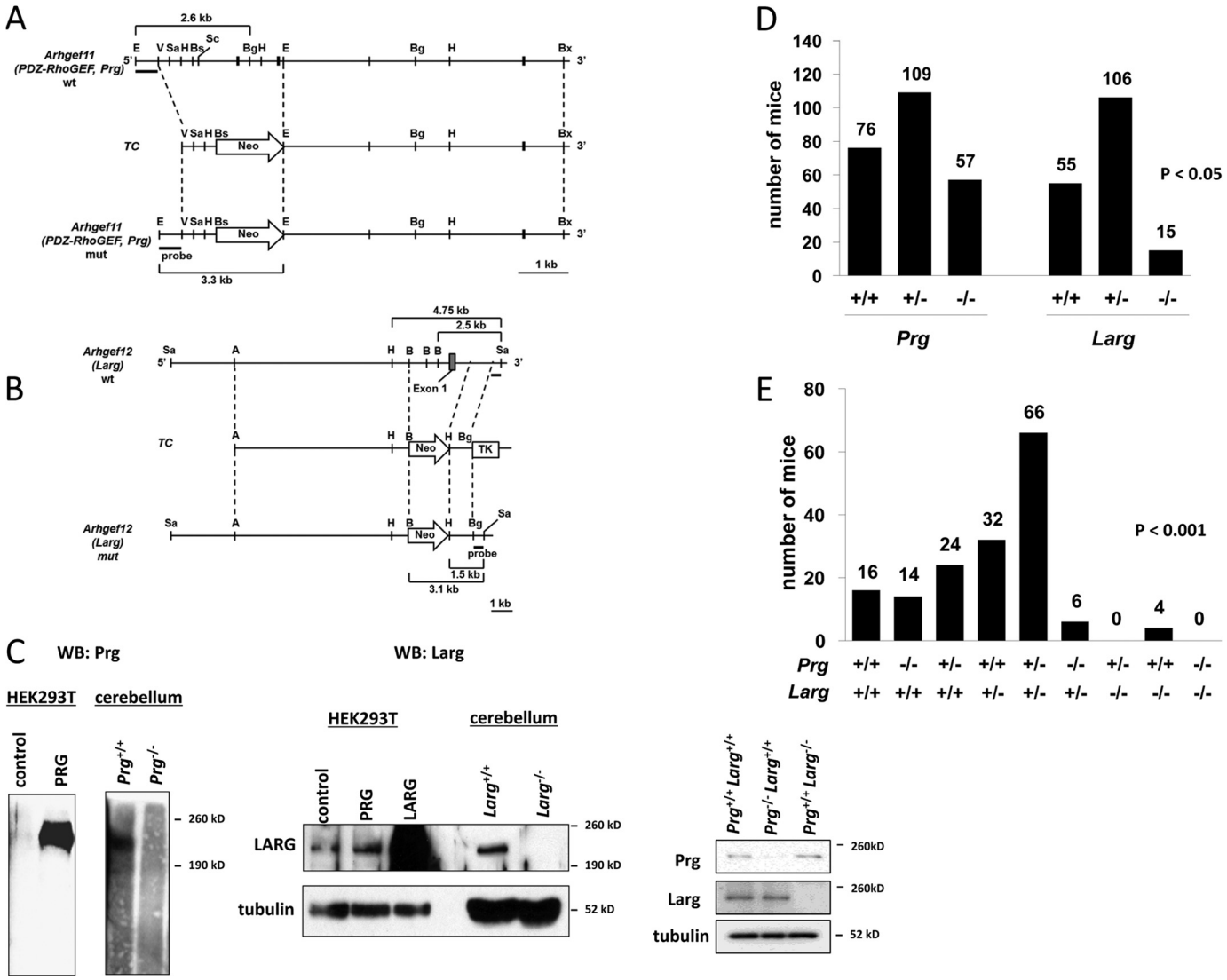

FIGURE 1. **Generation of PDZ-RhoGEF and LARG single and double-deficient mice.** *A* and *B*, targeted disruption of the murine *Arhgef11* (*PDZ-RhoGEF* or *Prg*, encoding PDZ-RhoGEF) (*A*) and *Arhgef12* (*Larg*, encoding LARG) (*B*) genes. Part of the wild type *Prg* (*A*) and *Larg* (*B*) locus (*wt*), the targeting construct (*TC*), and the targeted locus (*mut*) are shown. The wild type genes were disrupted by means of a targeting vector in which the second and third exon (*A*) and the first exon (*B*) were replaced by the neomycin resistance gene. *E*, EcoRI; *Sa*, SacI; *H*, HindIII; *Bs*, BsaI; *Sc*, ScaI; *Bg*, BglII. *C*, Western blots (*WB*) for Prg of cerebellum extracts from wild type and *Prg*-deficient mice (*left panel*) and for Larg of cerebellum extracts from wild type and *Larg*-deficient mice (*right panel*). The bands correspond to the molecular weight of the bands of PRG- and LARG-transfected HEK-293T cells respectively (corresponding controls). Mouse embryonic fibroblasts from *Prg*- and *Larg*-deficient mice were analyzed by Western blot for Prg and Larg. *D*, genotype distribution of offspring from interbred heterozygous *Prg* or *Larg* 21 days after birth. *E*, genotype distribution of offspring from interbred heterozygous *Prg* and *Larg* mice 21 days after birth.

by washing. Fresh serum-free medium with or without 0.1 unit/ml thrombin was added immediately. Phase contrast images of the wound were obtained after 24 h or every 20 min for live cell imaging. The uncovered wound area was calculated with AxioVision software (Carl Zeiss).

Live Cell Imaging—Live cell imaging was performed with an inverted Zeiss LSM 700 confocal microscope, as described previously (28).

Statistical Analysis—All of the experiments were repeated at least three times with similar results. Statistical analysis of number of vessels, cell proliferation, migration assay, and wound healing was performed by unpaired two-tailed Student's *t* test. The *asterisks* in the figures denote statistical significance (*NS*, not significant, $p > 0.05$; *, $p < 0.05$; **, $p < 0.01$; ***, $p < 0.001$).

RESULTS

Generation of Prg- and Larg-deficient Mice—To investigate the role of Prg and Larg in mammalian development and function, we targeted the *Arhgef11* (referred herein as *Prg*, encoding PDZ-RhoGEF or Prg) and *Arhgef12* (referred herein as *Larg*, encoding Larg) genes, in mouse embryonic stem cells for disruption by homologous recombination. *Prg* was targeted with a vector that resulted in the deletion of exons 2 and 3 (Fig. 1*A*). The vector that was generated to target the *Larg* gene deleted exon 1, including the promoter and transcriptional start site, and therefore abolished transcription of the *Larg* (Fig. 1*B*). When heterozygous mice were mated, we obtained both $Prg^{-/-}$ and $Larg^{-/-}$ mice. In a mixed 129/C57B6/J background, we could observe no obvious phenotype on either Prg-

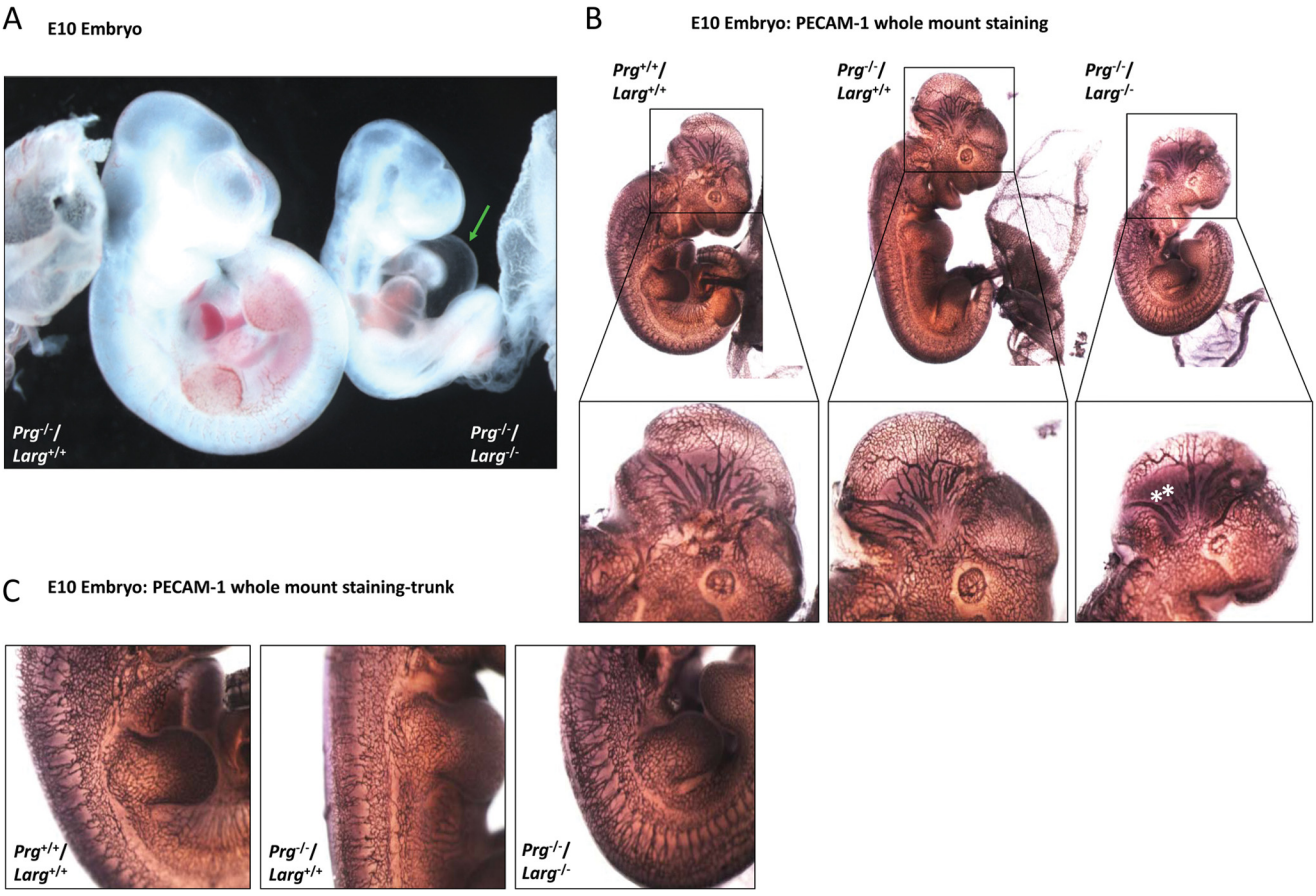

FIGURE 2. **Combined Prg- and Larg-deficient embryos are less developed with partial branching failure of the cranial vessels.** *A*, side view of *Prg* knock-out and double (*Prg* and *Larg*) knock-out E10 embryos. *B*, whole mount PECAM-1 staining of wild type, *Prg* knock-out, and double (*Prg* and *Larg*) knock-out E10 embryos. The magnified images show branching of the main cranial vessels of wild type, *Prg* knock-out, and double (*Prg* and *Larg*) knock-out E10 embryos. *C*, whole mount PECAM-1 staining of the trunk of wild type, *Prg* knock-out, and double (*Prg* and *Larg*) knock-out E10 embryos.

or Larg-deficient mice. Western blot analyses on adult tissues of wild type and Prg- and Larg-deficient mice demonstrated the absence of Prg or Larg protein in the respective knock-out mice (Fig. 1*C*). As a control, no compensatory changes were observed on Prg expression in MEFs isolated from $Larg^{-/-}$ mice or on Larg expression levels in fibroblasts derived from $Prg^{-/-}$ mice (Fig. 1*C* and see below). The distribution of the resulting genotypes after crossing *Prg* heterozygous mice was Mendelian (Fig. 1*D*). However, the distribution of the resulting genotypes from a cross of $Larg^{+/-}$ with $Larg^{+/-}$ mice was significantly different from the expected ratio, resulting in fewer Larg-deficient mice surviving to birth (Fig. 1*D*). Birth weight, adult weight, survival, behavior, and gross anatomy appeared no different in mice deficient in either gene when compared with wild type (data not shown). In particular for Larg, it seems that once the embryos survive past a crucial developmental checkpoint, this GEF is not required for vital functions in the adult mouse. Overall, the fact that mice deficient for Prg or Larg individually are viable suggests that these mice may survive because of a compensatory mechanism because both proteins have similar structure, and hence they may have redundant functions.

Therefore, to determine whether mice deficient for both Prg and Larg are viable, we crossed $Prg^{+/-}$ $Larg^{+/-}$ with $Prg^{+/-}$ $Larg^{+/-}$ mice to obtain mice deficient in both genes. Interestingly, the distribution of the resulting genotypes at weaning age was very different from the expected Mendelian ratio, because we could not obtain $Prg^{-/-}$ $Larg^{-/-}$ or $Prg^{+/-}$ $Larg^{-/-}$ mice, and we also obtained fewer $Prg^{-/-}$ $Larg^{+/-}$ and $Prg^{+/+}$ $Larg^{-/-}$ mice than expected. This implies that the presence of either Prg or Larg is required for vital functions during development.

Prg and Larg Double-deficient Mice Die during Midgestation—The embryonic lethality of Prg and Larg double-deficient mice prompted us to further investigate the potential developmental defects caused by *Prg* and *Larg* gene ablation. We dissected and genotyped embryos at various stages of development and observed that by E10.5 there were no surviving $Prg^{-/-}$ $Larg^{-/-}$ embryos (data not shown). At earlier stages of development, these embryos were present and alive, as assessed by the presence of a beating heart; however, these mouse embryos were phenotypically very different from their control littermates. Fig. 2*A* depicts the typical phenotype of the $Prg^{-/-}$ $Larg^{-/-}$ embryo at E10 day of development. The double-deficient embryos were smaller and less developed than their control littermates and had an enlarged pericardial sac. Furthermore, double-deficient embryos showed a defect in blood vessel distribution when compared with their control littermates (Fig. 2*A*). For example, blood vessel analysis by PECAM-1 whole mount staining of double-deficient embryos and their control littermates showed partial branching failure in two of six cranial vessels, resulting in

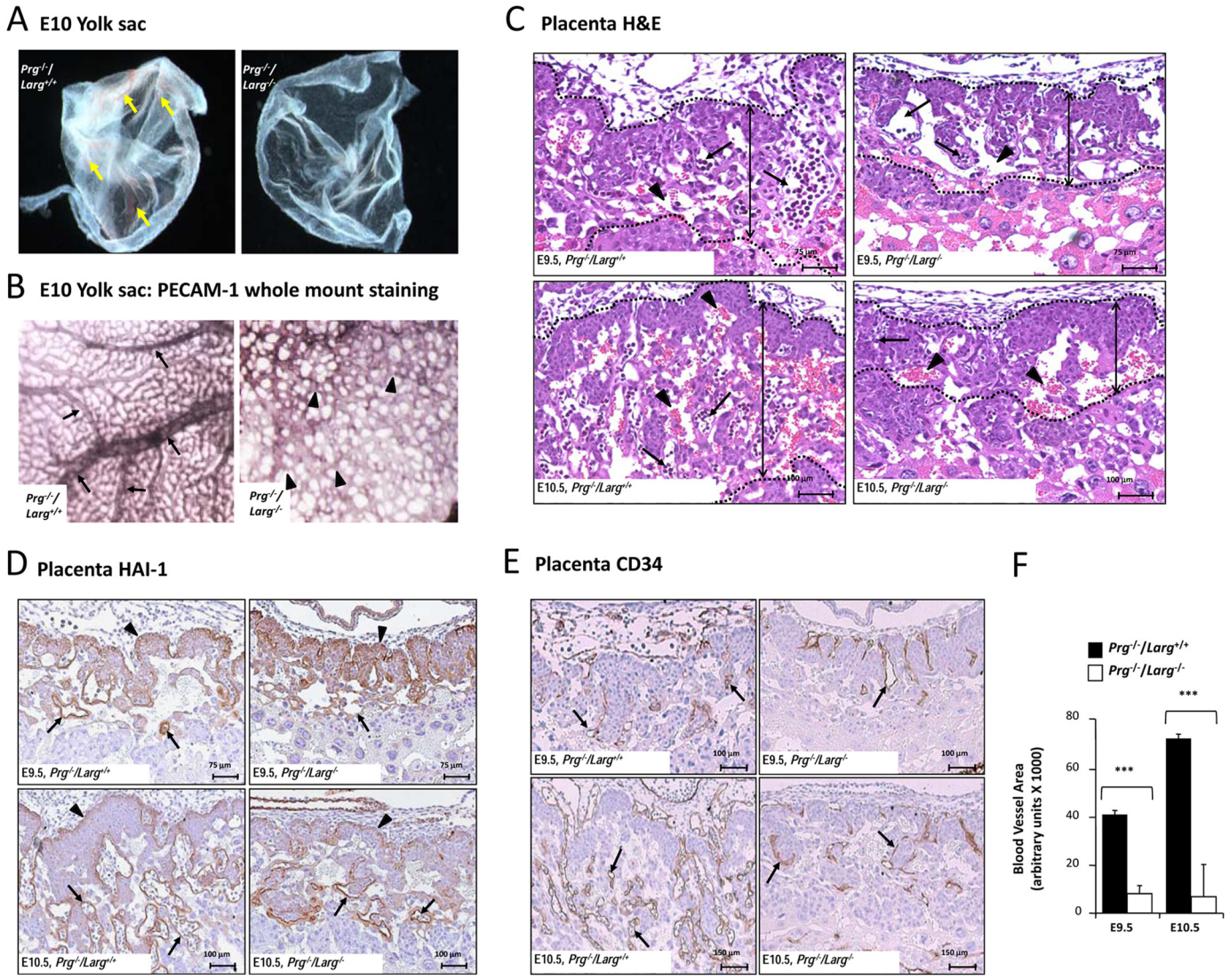

FIGURE 3. **Placentas of Prg and Larg double-deficient embryos are less developed and poorly vascularized.** *A*, untreated yolk sacs from wild type and double knock-out E10 embryos. Blood-containing vessels are present in the wild type yolk sac (*arrows*). *B*, whole mount PECAM-1 staining of yolk sacs from wild type and double knock-out E10 embryos. Organized, mature vessels are present in the yolk sacs of wild type embryos (*arrows*), *versus* disorganized and immature vasculature (*arrowheads*) in Prg and Larg double-deficient embryos. *C*, histological appearance of hematoxylin and eosin (*H&E*)-stained placental tissues of Prg single-deficient ($Prg^{-/-}/Larg^{+/+}$, *left panels*) and Prg/Larg double-deficient ($Prg^{-/-};Larg^{-/-}$, *right panels*) embryos at E9.5 (*top panels*) and E10.5 (*bottom panels*). The thickness of the placental labyrinth (*double-headed arrows* between the *dotted lines*) is reduced in double-deficient tissues. At E10.5, the complexity of the labyrinth, characterized by the number of fetal vessels (*arrows*) and lacunae filled with maternal blood (*arrowheads*) within the labyrinth is markedly reduced in Prg/Larg double-deficient, compared with Prg single-deficient tissues. *D*, immunohistochemical detection of the labyrinth marker HAI-1 in placental tissues of Prg single-deficient ($Prg^{-/-}/Larg^{+/+}$, *left panels*) and Prg/Larg double-deficient ($Prg^{-/-};Larg^{-/-}$, *right panels*) embryos at E9.5 (*top panels*) and E10.5 (*bottom panels*). Expression of HAI-1 is detected in stem cell-containing chorionic (*arrowheads*) and differentiated labyrinthine (*arrows*) trophoblasts. The population of differentiated trophoblasts is not significantly different in Prg/Larg double-deficient, compared with Prg single-deficient tissues. *E*, immunohistochemical detection of endothelial cell marker CD34 in placental tissues of Prg single-deficient ($Prg^{-/-}/Larg^{+/+}$, *left panels*) and Prg/Larg double-deficient ($Prg^{-/-};Larg^{-/-}$, *right panels*) embryos at E9.5 (*top panels*) and E10.5 (*bottom panels*). The number of fetal vessels (*arrows*) within the placental labyrinth is strongly reduced in Prg/Larg double-deficient tissues, compared with Prg single-deficient tissues at both E9.5 and E10.5. *F*, quantification of the number of fetal vessels in the placental labyrinth of Prg single-deficient ($Prg^{-/-}/Larg^{+/+}$, *black bars*) and Prg/Larg double-deficient ($Prg^{-/-};Larg^{-/-}$, *white bars*) embryos at E9.5 and 10.5. Fetal vessel density was strongly diminished in double-deficient mice.

less overall vessel branching in the head (Fig. 2*B*). However, vessel branching in the trunk did not show an obvious abnormality (Fig. 2*C*). The developmental stage at which double-deficient embryos die, in combination with the above phenotypic observations, suggest that the dying embryos may exhibit multiple and complex vascular defects.

Prg and Larg Are Required for Normal Vascular Development in Yolk Sacs and Placentas—The smaller size of the double-deficient embryos prompted us to investigate whether the decrease in development was also due to a deficiency in blood vessel formation in the yolk sac and in the placenta. Yolk sacs from E10 *Prg* and *Larg* double-deficient mice showed less visible blood vessels when compared with their control littermates (Fig. 3*A*). PECAM-1 whole mount staining of E10 yolk sacs from double-deficient embryos displayed a disorganized and less developed vascular plexus with dilated, not well oriented vessels (Fig. 3*B*).

Histological analysis of placentas stained with hematoxylin and eosin revealed that the labyrinth, which represents the embryonic and maternal interface, was markedly thinner in the

double-deficient placentas compared with the *Prg*$^{-/-}$ *Larg*$^{+/+}$ or the wild type placentas (Fig. 3*C* and supplemental Fig. S1*A*). The morphology of the trophoblast layers appeared to be normal in the double-deficient placentas, but there were significantly fewer embryonic primitive erythrocytes present. The embryonic erythrocytes at this stage are still nucleated, which makes it easy to distinguish them from maternal erythrocytes. The thinner labyrinth and fewer blood vessels containing embryonic hematopoietic cells led us to perform a more detailed histological analysis of the placenta to elucidate any trophoblast proliferation or differentiation defects. Placental cells are normally proliferating very actively as the embryo grows. Staining of placentas from E9.5 and E10.5 embryos for a proliferation marker, proliferating cell nuclear antigen, showed no significant difference in embryonic trophoblast growth (supplemental Fig. S1*B*). Chorionic trophoblasts differentiate to form the layers of the labyrinth that invade toward the maternal spongial layer. This enables the development of embryonic vascular networks required for nutrient and oxygen exchange with the nearby maternal vasculature. In this regard, HAI-1 is a protein expressed in chorionic trophoblasts and the more differentiated syncytiotrophoblasts (29), and it did not appear to be altered in double-deficient placentas (Fig. 3*D*). Together, it appears that the proliferation and differentiation of the placental trophoblast layers are not affected by combined deletion of *Prg* and *Larg*, suggesting the placental labyrinth phenotype may be due to a vascular defect.

The lack of embryonic erythrocytes in the embryonic portion of the placentas from double-deficient embryos could indicate a vascular or hematopoietic defect. Expression of the endothelial stem cell marker CD34 clearly outlined the lumens of the vasculature in placentas from *Prg*$^{+/+}$ *Larg*$^{+/+}$, *Prg*$^{-/-}$ *Larg*$^{+/+}$, and double-deficient embryos (Fig. 3*E* and supplemental Fig. S1*A*). However, the vascular staining revealed a reduction of the number of vessels present in the labyrinth within the double-deficient placentas, as compared with *Prg*$^{-/-}$ *Larg*$^{+/+}$ mice. This deficiency was even more prominent at day E10.5 (Fig. 3*E* and supplemental Fig. S1*A*), which suggests that the placentas of the double-deficient embryos do not develop the requisite vascular network, which likely starves the growing and invading embryonic tissue. The above observations, combined with the deficiencies in the vascular plexus development of the double-deficient embryos, may each contribute to embryonic lethality during midgestation.

Impact of Combined Prg, Larg, and p115 Deficiency on Thrombin-induced Activation of RhoA—We next isolated MEFs from deficient for Prg-deficient, Larg-deficient, double-deficient, and wild type mouse embryos to delineate the effect of the absence of Prg and Larg at the cellular level. MEFs wild type and double-deficient for Prg and Larg were also infected with lentiviruses that expressed either empty vector (pLKO1) or vector containing two shRNA sequences for p115. After selection with puromycin, the cells were lysed, and Western blots were performed to monitor the expression of all three GEFs. As positive controls, HEK-293T cells were transfected with constructs expressing GFP fused to human PRG, LARG, and p115, and lysates were analyzed by Western blot and probed with the corresponding antibodies (Fig. 4). As expected,

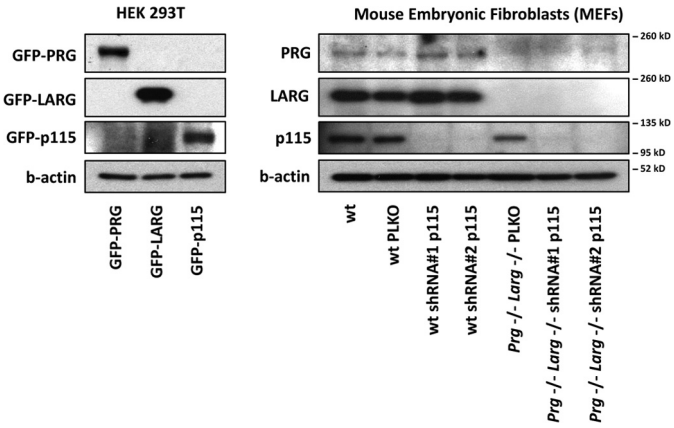

FIGURE 4. **Generation of mouse embryonic fibroblasts from wild type and Prg and Larg double-deficient mice.** Shown are Western blots for PRG, LARG, p115 GEF, and β-actin of HEK-293T cell extracts overexpressing PRG, LARG, and p115 (*left panel*) and of mouse embryonic fibroblast extracts from wild type (*wt*) and Prg and Larg double-deficient mice (−/−), infected either with the vector (pLKO1) or shRNA for p115 (*right panel*).

MEFs isolated from mice double-deficient for Prg and Larg did not express these GEFs. Furthermore, both shRNA sequences for p115 reduced the expression of this GEF below the detection limit in both Prg and Larg double-deficient and wild type MEFs (Fig. 4).

Prg, Larg, and p115 are able to stimulate RhoA activation (13, 30, 31). We wanted to explore which of these GEFs contributes to RhoA activation downstream of $G\alpha_{12/13}$ ligands. We therefore performed time course experiments with thrombin stimulation, which acts by activating PAR-1, a GPCR that stimulates primarily $G\alpha_{12/13}$ and $G\alpha_i$ (26, 32, 33), followed by Rho pulldowns and Western blots for RhoA (Fig. 5*A*). Thrombin induced a rapid increase of RhoA activation in wild type MEFs, as well as in MEFs infected with the shRNA empty vector (PLKO). Knockdown of p115 led to a decrease of RhoA activation; however, a much more robust inhibition was obtained in the case of the MEFs doubly deficient for Prg and Larg. Finally, knockdown of p115 in the double-deficient MEFs almost completely abolished thrombin-induced RhoA activation. Quantification of RhoA activation 3 min after thrombin addition, a time point that represents the maximal response, showed that all three GEFs contribute to RhoA activation, with Prg and Larg playing a major role (Fig. 5*B*). Similar findings were also observed for LPA, which stimulates $G\alpha_{12/13}$ potently (supplemental Fig. S2, *A* and *B*). To explore whether Prg, Lrg, and p115 also contribute to G_q signaling to Rho, we tested a selected panel of agonists that act primarily through endogenous $G\alpha_q$-coupled receptors and performed RhoA pulldown experiments. From these, bradykinin and endothelin were the most potent to induce RhoA activation, as judged by dose-response experiments (supplemental Fig. S3). Of interest, time course analysis with bradykinin and endothelin using both wild type and Prg and Larg double-deficient MEFs in which p115 was knocked down revealed that RhoA activation by polypeptides acting on endogenous $G\alpha_q$-coupled receptors is not dependent on the presence of these RhoGEFs (Fig. 5*C*).

Role of Prg, Larg, and p115 in Cell Proliferation—Thrombin induces multiple signaling events in fibroblasts resulting in cell proliferation (32). Thus, we asked whether the absence of

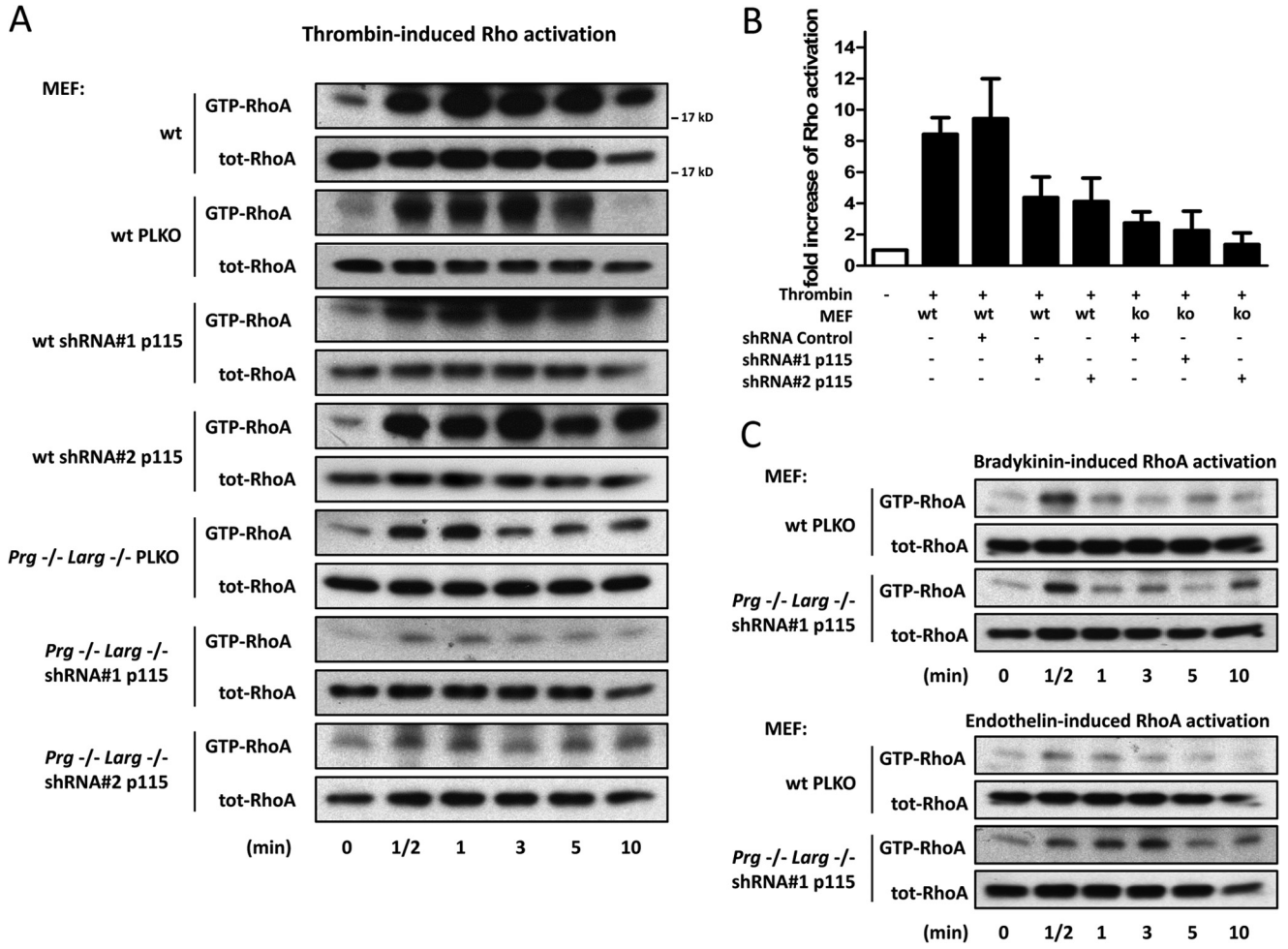

FIGURE 5. **Thrombin-induced RhoA activation through $G\alpha_{12/13}$ is dependent on the expression of Prg, Larg, and p115.** *A*, time course experiments of thrombin (0.1 unit/ml) stimulation in mouse embryonic fibroblasts from wild type (*wt*) and double knock-out (−/−) for *Prg* and *Larg* mice, infected either with the vector (pLKO1) or shRNA for p115. Active RhoA was identified from the lysates through incubation with GST-RBD beads, as described under "Experimental Procedures," and both active and total RhoA were assessed by Western blotting against RhoA. *B*, the data represent RhoA activation 3 min after thrombin stimulation in each mouse embryonic fibroblast cell line, are expressed as fold induction in respect to the same cells prior stimulation, and are the means ± S.E. of at least three independent experiments. *C*, time course experiments of bradykinin (*upper panels*) and endothelin (*lower panels*) stimulation in mouse embryonic fibroblasts from wild type mice infected with the vector (pLKO1) and double knock-out (−/−) for *Prg* and *Larg* mice, infected with shRNA for p115. Active RhoA was identified from the lysates through incubation with GST-RBD beads (see "Experimental Procedures"), and both active and total RhoA were assessed by Western blotting against RhoA.

expression of Prg, Larg, and p115 would have an impact on the proliferation of MEFs, by using an EdU incorporation assay. The basal proliferation levels of MEFs from Prg and Larg double-deficient mice were much lower than wild type MEFs, irrespectively of whether p115 was knocked down or not. Thrombin was able to potently stimulate the proliferation of wild type MEFs, reaching a more than 2-fold increase in DNA synthesis, similar to serum-treated cells. However, thrombin failed to increase the proliferation in cells lacking Prg and Larg, or all three RSG-containing RhoGEFs, despite these cells still responding to serum as an internal control (Fig. 6, *A* and *B*).

RhoA activation downstream of $G\alpha_{12/13}$ receptors can initiate multiple biological functions through the activation of p38 and JNK MAPKs (7). Indeed, thrombin activation caused a potent induction of p38 and JNK phosphorylation in wild type MEFs (Fig. 6*C*). This was nearly abolished in MEFs lacking all three RGS-containing RhoGEFs (Fig. 6*C*). Similarly, in wild type MEFs, where endogenous levels of pJNK were not detectable, thrombin induced a robust activation of JNK, but not in MEFs where the three GEFs were not expressed (Fig. 6*D*). Each of these GEFs play a role in the activation of p38 and JNK because Larg or Prg deficiency, or p115 knockdown, each reduced partially the activation of these MAPKs (data not shown). Finally, thrombin-induced activation of ERKs was not substantially affected after genetic deletion of *Larg* and *Prg* and p115 knockdown (Fig. 6*E*).

Prg, Larg, and p115 Are Required for Thrombin-induced Cell Retraction, Migration, and Wound Healing—One of the typical downstream $G_{12/13}$ signaling effects caused by thrombin in cells is the polymerization of G actin to F actin, which contributes to cell migration (7, 26). A 17-amino acid peptide (Lifeact) is able to bind filamentous actin (F-actin) structures in eukaryotic cells without interfering with actin dynamics *in vivo* and *in vitro*, and hence its C-terminal GFP fusion represents a suitable tool for staining F-actin changes using live cell imaging (34). We therefore transfected wild type MEFs and cells singly and doubly deficient in Prg and Larg with p115 knockdown with Lifeact-GFP and visualized F-actin changes after thrombin stimulation

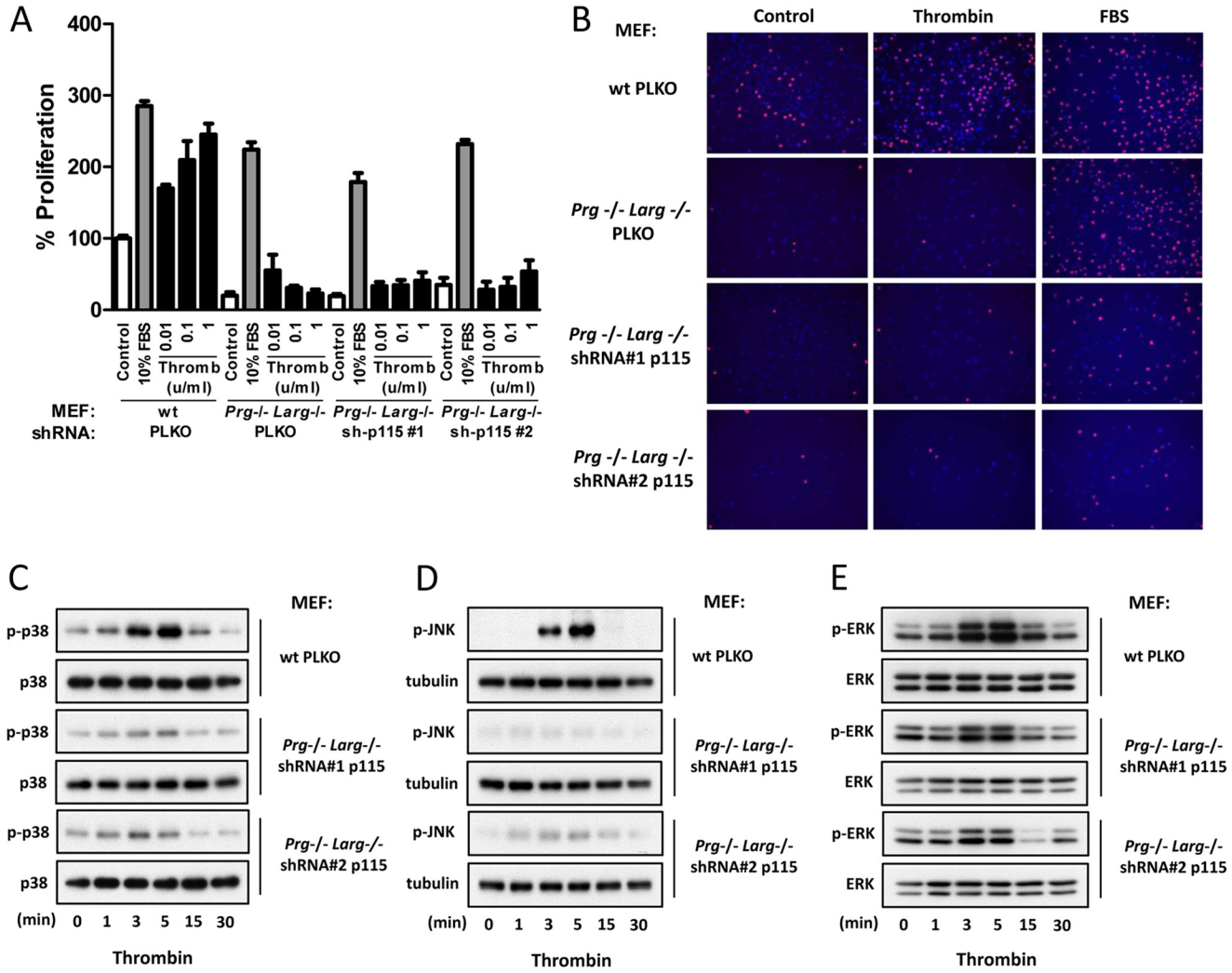

FIGURE 6. **p38 and JNK activation is markedly reduced in absence of Prg, Larg, and p115, as well as basal and thrombin-induced cell proliferation.** *A*, cell proliferation was assessed in mouse embryonic fibroblasts from wild type mice infected with vector (pLKO1) and from Prg and Larg double-deficient mice infected either with vector (pLKO1) or shRNA for p115. The cells were treated with various concentrations of thrombin and analyzed for cell proliferation by the Click-iT assay. The data represent percentages of proliferation with respect to control cells (mouse embryonic fibroblasts from wild type (*wt*) mice), and the means ± S.E. of triplicate samples from a typical experiment are shown. *B*, representative images of the proliferating cells. EdU-stained nuclei (*red*) correspond to the proliferating cells, DAPI (*blue*) stained all nuclei. *C–E*, Western blots demonstrating p38 (*C*), JNK (*D*), and pERK (*E*) activation in thrombin-induced time course stimulation of mouse embryonic fibroblasts from wild type mice infected with the vector (pLKO1) and double-deficient mice for Prg and Larg, infected with shRNA for p115.

(Fig. 7*A*). The basal state of actin polymerization was not consistently altered in the distinct MEF populations used for the analysis (supplemental Fig. S4). Remarkably, cells lacking all three RhoGEFs did not show changes in F-actin formation, and they did not retract after thrombin stimulation, in contrast to the remarkable effect of thrombin on wild type MEFs (Fig. 7*A*). We also tested potential differences on cell migration in wild type and MEFs defective for RhoGEFs using a Boyden chamber migration assay. As shown in Fig. 7*B*, the spontaneous migration of the wild type MEFs was much higher than those of MEFs that do not express the three RhoGEFs. Furthermore, thrombin stimulation caused a more than 2-fold increase of cell migration in the case of wild type MEFs, whereas it did not affect the migration levels of the double Prg and Larg-deficient MEFs with down-regulated p115.

We studied the behavior of the wild type MEFs and cells that do not express Prg, Larg, and p115 in wound healing assays, which allow the study of the combination of cell migration with cell-cell and cell matrix interactions and found out that only wild type MEFs are able to initiate wound closure after 48 h (Fig. 7*C*). Thrombin stimulation expedited the gap closure in the case of wild type MEFs. Fig. 7*D* and supplemental Fig. S5 (see also supplemental Movies S4 and S5) show representative pictures after cell wounding and 48 h later.

DISCUSSION

Multiple important roles have been attributed to $G\alpha_{12/13}$-coupled Rho GEFs; however, their precise biological functions *in vivo* are far from being characterized. We now show that mice deficient for Prg or Larg are viable with no overt phenotypes. However, Larg-deficient mice displayed embryonic lethality with incomplete penetrance, suggesting that Larg expression is required during development and that its loss may impact animal viability. Interestingly, deficiency for both Prg and Larg, however, leads to embryonic lethality during midgestation. Prg and Larg double-deficient mice demonstrate multi-

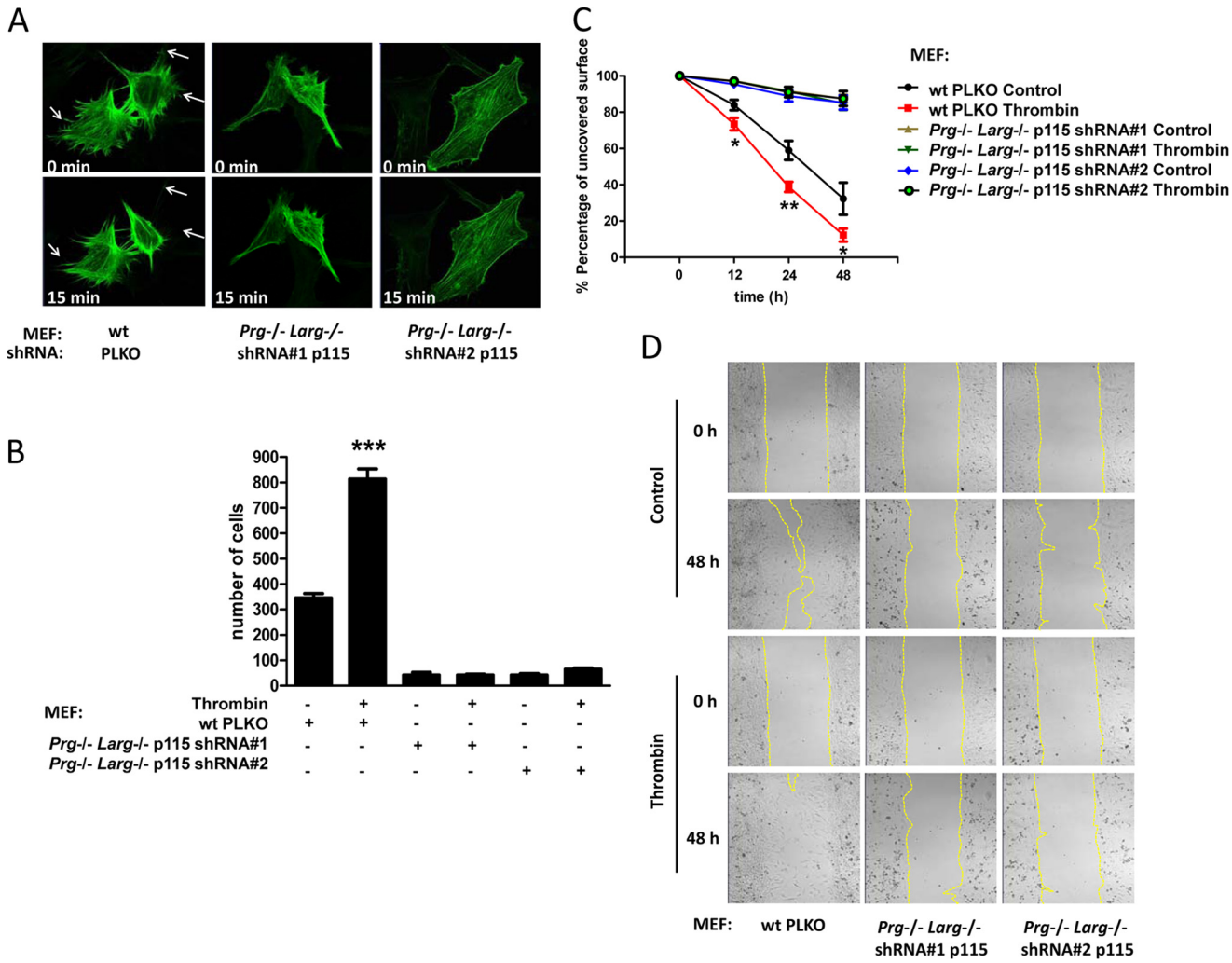

FIGURE 7. **Thrombin-induced cell retraction and basal and thrombin-induced migration and wound healing are markedly reduced by the combined absence of Prg, Larg and p115.** *A*, evaluation of thrombin-induced retraction of mouse embryonic fibroblasts from wild type (*wt*) mice infected with the vector (pLKO1) and from Prg and Larg double-deficient mice, infected with shRNA for p115. Representative pictures were taken before (0 min) and after (15 min) thrombin stimulation or every 20 s for live cell imaging (supplemental Movie S1, WT pLKO1; supplemental Movie S2, $Prg^{-/-}$ $Larg^{-/-}$ shRNA#1 p115; and supplemental Movie S3, $Prg^{-/-}$ $Larg^{-/-}$ shRNA#2 p115). *B*, mouse embryonic fibroblasts from wild type mice infected with the vector (pLKO1) and from double-deficient for Prg and Larg mice (−/−) infected with shRNA for p115 were tested for migration in the absence or presence of thrombin (0.1 unit/ml), as described under "Experimental Procedures." The cell numbers were quantified using an optical microscope. *C*, mouse embryonic fibroblasts from wild type mice infected with the vector (pLKO1) and from Prg and Larg double-deficient (−/−) mice infected with shRNA for p115 were tested in wound healing assay in the absence or presence of thrombin (0.1 unit/ml), as described under "Experimental Procedures." The measurements were performed 12, 24, and 48 h after wounding. *D*, representative pictures shown were obtained right after the wounding (0 h) and 48 h later or every 20 min for live cell imaging.

ple and complex vascular alterations, including branching defects in cranial vessels. The gross anatomical and histological analysis of their yolk sac and placenta revealed the absence of vessels, without concomitant alteration of the trophoblast layer, suggesting that the angiogenic defects are present in the entire embryo and may contribute to the early lethality of these mice. Overall, these findings suggest that Prg and Larg double deficiency results in a complex series of embryonic and placental defects and support an essential role for these GEFs in mouse development.

Some *Prg*/*Larg* KO embryos die at E10.5, 1 day later than $G\alpha_{12}$ and $G\alpha_{13}$ double-deficient mice, most of which die at E9.0-E9.5 (26, 35). This may be explained based on a partial redundancy of p115 during development, which may compensate for the loss of Prg and Larg in a variable fashion, depending on its expression level in each cell type and tissue at different developmental stage. In addition, embryos deficient in $G\alpha_{12}$ and $G\alpha_{13}$ die primarily from a major defect in angiogenesis (35), but mice lacking Prg and Larg appear to have broader developmental alterations. These multiple developmental defects observed here may result from the role of Prg and Larg in Rho activation by $G\alpha_{12/13}$ G protein subunit, as well as from their contribution to Rho signaling by other cell surface molecules in addition to GPCRs. For example, LARG can form a complex with insulin-like growth factor-1 receptor through its PDZ domain (19). Similarly, the PDZ domains of PRG and LARG interact with the PDZ-binding motif located at the C termini of Plexin-B family members, and this interaction mediates RhoA activation and downstream signaling events involving axonal guidance, growth cone collapse, and endothelial cell migration (16, 17, 27). In addition, other domains within PRG and LARG can contribute to the assembly of plexin-associated signaling

complexes. For example, activation of Plexin-B1 by Sema4D and its subsequent tyrosine phosphorylation by HER2 create docking sites for the SH2 domains of phospholipase Cγ, which is recruited into the complex and activates PRG through its SH3 domain (36). The interaction between PRG and Plexin-B1 is also promoted by Rnd1, a member of the Rho family of GTPases, which regulates RhoA activation downstream of Plexin-B1 signaling (37). In vascular smooth muscle cells, angiotensin II stimulates PYK2 association with tyrosine-phosphorylated PRG, which leads to Rho/ROCK activation and cell migration, providing a mechanistic role of PRG and Rho pathway on vascular remodeling (38). In the same cells, angiotensin II up-regulates LARG expression via the AT1 receptor, thus playing a role in RhoA activation (39). Thus, the complex phenotype of embryos deficient for both Prg and Larg may result from the multiple functions of these GEFs in signal transmission in addition to their best known role in G protein signaling.

The zebrafish homolog of PRG is expressed ubiquitously at the blastula and gastrula stages and enriched in neural tissues later in embryogenesis where it stimulates actin stress fiber formation (40). Loss of function experiments led to embryos with ventrally curved axes and other phenotypes associated with ciliated epithelia, establishing a role for Prg in ciliated epithelia during vertebrate development (40). Prg has been also shown to participate in neural tube closure, a critical step of embryogenesis, and to cooperate with Celsr1, Dishevelled, and DAAM1 in the adherens junctions oriented toward the mediolateral axes of the bending neural plates (41). This interaction leads to actomyosin-dependent contraction in a planar-polarized manner that promotes simultaneous apical constriction and midline convergence of myoepithelial cells (41). In light of these and other studies, it was surprising to find that Prg-deficient mice are viable and do not exhibit any overt phenotype. We also did not observe a shorter life span of *Prg* KO mice.[8] This suggests that many of the functions assigned to Prg thus far may be compensated in mammalian cells by Larg, given its similar protein domain structure and widespread tissue distribution. However, this may not be strictly the case regarding the compensation of Larg deficiency by Prg, because Larg-deficient mice are born with a much lower frequency than would be expected. Thus, we can speculate that Prg and Larg may perform specific functions in adults but that during development Larg can compensate for the absence of Prg protein. Instead, Prg expression may not be sufficient to fully rescue the absence of Larg for some critical, yet to be defined developmental stage, leading to fewer surviving mice that may have bypassed the likely more Larg-dependent developmental processes. This, as well as the possibility of the existence of Larg-specific functions in adults, may warrant further investigation.

G$\alpha_{12/13}$-coupled receptors regulate many important biological processes, from embryonic development to platelet activation, smooth muscle contraction, immune responses, and cancer metastasis (7, 33). Whereas Gα_{12}-deficient mice are normal, mice deficient for Gα_{13} die at embryonic day 9.5, because of angiogenic defects (26). Many downstream targets for Gα_{12} and/or Gα_{13} have been identified, including Rho GEFs, RGS proteins, cadherins, radixin, nonreceptor tyrosine kinases of the Src family, protein phosphatases, zonula occludens 1 and 2, and Hsp90 (42). Among the candidate Rho GEFs regulated by Gα_{12} and Gα_{13}, PRG, LARG, p115, and Lbc are widely expressed in the mammals (8), with PRG being expressed higher in the central nervous system (43) and the chimeric protein protein AKAP-Lbc being highly expressed in the heart (14). We show here that Prg and Larg are essential for embryonic development and that these GEFs play a major role in Rho stimulation in response to thrombin and LPA, which activate Gα_{12} and Gα_{13}. In addition, fibroblasts deficient in Prg and Larg and knocked down for p115 revealed that these GEFs are required to stimulate Rho by PAR-1 and LPA receptors, respectively, but not for the activation of Rho by endogenous receptors that specifically activate Gα_q. Furthermore, despite the multiple molecular candidates mediating the growth and migratory activity elicited by Gα_{12}-coupled GPCRs, we show here that these three RGS-containing GEFs are essential for the activation of signaling transduction pathways linking thrombin receptors to the nucleus through JNK and p38 and for promoting the rearrangement of the cytoskeleton, thereby initiating cell motility. Overall, our findings identified an essential function for Prg and Larg for animal development and support the critical role of Prg and Larg in signaling to Rho downstream of G$\alpha_{12/13}$-coupled receptors. This provides further evidence of the key role of the Prg/Larg-Rho signaling axis in the regulation of cell migration and proliferation by G$\alpha_{12/13}$-linked GPCRs.

Acknowledgment—We thank Dr. Roberto Weigert (NIDCR, National Institutes of Health) for providing the Lifeact plasmid.

[8] C. M. Mikelis, T. R. Palmby, M. Simaan, W. Li, R. Szabo, R. Lyons, D. Martin, H. Yagi, S. Fukuhara, H. Chikumi, R. Galisteo, Y. Mukouyama, T. H. Bugge, and J. S. Gutkind, unpublished observation.

REFERENCES

1. Jaffe, A. B., and Hall, A. (2005) Rho GTPases. Biochemistry and biology. *Annu. Rev. Cell Dev. Biol.* **21,** 247–269
2. Heasman, S. J., and Ridley, A. J. (2008) Mammalian Rho GTPases. New insights into their functions from *in vivo* studies. *Nat. Rev. Mol. Cell Biol.* **9,** 690–701
3. Coso, O. A., Chiariello, M., Yu, J. C., Teramoto, H., Crespo, P., Xu, N., Miki, T., and Gutkind, J. S. (1995) The small GTP-binding proteins Rac1 and Cdc42 regulate the activity of the JNK/SAPK signaling pathway. *Cell* **81,** 1137–1146
4. Iden, S., and Collard, J. G. (2008) Crosstalk between small GTPases and polarity proteins in cell polarization. *Nat. Rev. Mol. Cell Biol.* **9,** 846–859
5. Rossman, K. L., Der, C. J., and Sondek, J. (2005) GEF means go. Turning on RHO GTPases with guanine nucleotide-exchange factors. *Nat. Rev. Mol. Cell Biol.* **6,** 167–180
6. Aittaleb, M., Boguth, C. A., and Tesmer, J. J. (2010) Structure and function of heterotrimeric G protein-regulated Rho guanine nucleotide exchange factors. *Mol. Pharmacol.* **77,** 111–125
7. Dorsam, R. T., and Gutkind, J. S. (2007) G-protein-coupled receptors and cancer. *Nat. Rev. Cancer* **7,** 79–94
8. Fukuhara, S., Chikumi, H., and Gutkind, J. S. (2001) RGS-containing RhoGEFs. The missing link between transforming G proteins and Rho? *Oncogene* **20,** 1661–1668
9. Diviani, D., Soderling, J., and Scott, J. D. (2001) AKAP-Lbc anchors protein kinase A and nucleates Gα_{12}-selective Rho-mediated stress fiber formation. *J. Biol. Chem.* **276,** 44247–44257
10. Vanni, C., Mancini, P., Ottaviano, C., Ognibene, M., Parodi, A., Merello, E., Russo, C., Varesio, L., Zheng, Y., Torrisi, M. R., and Eva, A. (2007) Gα_{13}

regulation of proto-Dbl signaling. *Cell Cycle* **6,** 2058–2070
11. Jin, S., and Exton, J. H. (2000) Activation of RhoA by association of $G\alpha_{13}$ with Dbl. *Biochem. Biophys. Res. Commun.* **277,** 718–721
12. Meiri, D., Greeve, M. A., Brunet, A., Finan, D., Wells, C. D., LaRose, J., and Rottapel, R. (2009) Modulation of Rho guanine exchange factor Lfc activity by protein kinase A-mediated phosphorylation. *Mol. Cell. Biol.* **29,** 5963–5973
13. Hart, M. J., Jiang, X., Kozasa, T., Roscoe, W., Singer, W. D., Gilman, A. G., Sternweis, P. C., and Bollag, G. (1998) Direct stimulation of the guanine nucleotide exchange activity of p115 RhoGEF by $G\alpha_{13}$. *Science* **280,** 2112–2114
14. Siehler, S. (2009) Regulation of RhoGEF proteins by $G_{12/13}$-coupled receptors. *Br. J. Pharmacol.* **158,** 41–49
15. Nourry, C., Grant, S. G., and Borg, J. P. (2003) PDZ domain proteins. Plug and play! *Sci. STKE* 2003, RE7
16. Perrot, V., Vazquez-Prado, J., and Gutkind, J. S. (2002) Plexin B regulates Rho through the guanine nucleotide exchange factors leukemia-associated Rho GEF (LARG) and PDZ-RhoGEF. *J. Biol. Chem.* **277,** 43115–43120
17. Swiercz, J. M., Kuner, R., Behrens, J., and Offermanns, S. (2002) Plexin-B1 directly interacts with PDZ-RhoGEF/LARG to regulate RhoA and growth cone morphology. *Neuron* **35,** 51–63
18. Yamada, T., Ohoka, Y., Kogo, M., and Inagaki, S. (2005) Physical and functional interactions of the lysophosphatidic acid receptors with PDZ domain-containing Rho guanine nucleotide exchange factors (RhoGEFs). *J. Biol. Chem.* **280,** 19358–19363
19. Taya, S., Inagaki, N., Sengiku, H., Makino, H., Iwamatsu, A., Urakawa, I., Nagao, K., Kataoka, S., and Kaibuchi, K. (2001) Direct interaction of insulin-like growth factor-1 receptor with leukemia-associated RhoGEF. *J. Cell Biol.* **155,** 809–820
20. Chikumi, H., Fukuhara, S., and Gutkind, J. S. (2002) Regulation of G protein-linked guanine nucleotide exchange factors for Rho, PDZ-RhoGEF, and LARG by tyrosine phosphorylation. Evidence of a role for focal adhesion kinase. *J. Biol. Chem.* **277,** 12463–12473
21. Chikumi, H., Barac, A., Behbahani, B., Gao, Y., Teramoto, H., Zheng, Y., and Gutkind, J. S. (2004) Homo- and hetero-oligomerization of PDZ-RhoGEF, LARG and p115RhoGEF by their C-terminal region regulates their *in vivo* Rho GEF activity and transforming potential. *Oncogene* **23,** 233–240
22. Booden, M. A., Siderovski, D. P., and Der, C. J. (2002) Leukemia-associated Rho guanine nucleotide exchange factor promotes $G\alpha_q$-coupled activation of RhoA. *Mol. Cell. Biol.* **22,** 4053–4061
23. Girkontaite, I., Missy, K., Sakk, V., Harenberg, A., Tedford, K., Pötzel, T., Pfeffer, K., and Fischer, K. D. (2001) Lsc is required for marginal zone B cells, regulation of lymphocyte motility and immune responses. *Nat. Immunol.* **2,** 855–862
24. Wirth, A., Benyó, Z., Lukasova, M., Leutgeb, B., Wettschureck, N., Gorbey, S., Orsy, P., Horváth, B., Maser-Gluth, C., Greiner, E., Lemmer, B., Schütz, G., Gutkind, J. S., and Offermanns, S. (2008) G_{12}-G_{13}-LARG-mediated signaling in vascular smooth muscle is required for salt-induced hypertension. *Nat. Med.* **14,** 64–68
25. Bugge, T. H., Flick, M. J., Daugherty, C. C., and Degen, J. L. (1995) Plasminogen deficiency causes severe thrombosis but is compatible with development and reproduction. *Genes Dev.* **9,** 794–807
26. Offermanns, S., Mancino, V., Revel, J. P., and Simon, M. I. (1997) Vascular system defects and impaired cell chemokinesis as a result of $G\alpha_{13}$ deficiency. *Science* **275,** 533–536
27. Basile, J. R., Barac, A., Zhu, T., Guan, K. L., and Gutkind, J. S. (2004) Class IV semaphorins promote angiogenesis by stimulating Rho-initiated pathways through plexin-B. *Cancer Res.* **64,** 5212–5224
28. Yagi, H., Tan, W., Dillenburg-Pilla, P., Armando, S., Amornphimoltham, P., Simaan, M., Weigert, R., Molinolo, A. A., Bouvier, M., and Gutkind, J. S. (2011) A synthetic biology approach reveals a CXCR4-G_{13}-Rho signaling axis driving transendothelial migration of metastatic breast cancer cells. *Sci. Signal.* **4,** ra60
29. Szabo, R., Molinolo, A., List, K., and Bugge, T. H. (2007) Matriptase inhibition by hepatocyte growth factor activator inhibitor-1 is essential for placental development. *Oncogene* **26,** 1546–1556
30. Fukuhara, S., Chikumi, H., and Gutkind, J. S. (2000) Leukemia-associated Rho guanine nucleotide exchange factor (LARG) links heterotrimeric G proteins of the G_{12} family to Rho. *FEBS Lett.* **485,** 183–188
31. Fukuhara, S., Murga, C., Zohar, M., Igishi, T., and Gutkind, J. S. (1999) A novel PDZ domain containing guanine nucleotide exchange factor links heterotrimeric G proteins to Rho. *J. Biol. Chem.* **274,** 5868–5879
32. Coughlin, S. R. (2000) Thrombin signalling and protease-activated receptors. *Nature* **407,** 258–264
33. Worzfeld, T., Wettschureck, N., and Offermanns, S. (2008) G_{12}/G_{13}-mediated signalling in mammalian physiology and disease. *Trends Pharmacol. Sci.* **29,** 582–589
34. Riedl, J., Crevenna, A. H., Kessenbrock, K., Yu, J. H., Neukirchen, D., Bista, M., Bradke, F., Jenne, D., Holak, T. A., Werb, Z., Sixt, M., and Wedlich-Soldner, R. (2008) Lifeact. A versatile marker to visualize F-actin. *Nat. Methods* **5,** 605–607
35. Gu, J. L., Müller, S., Mancino, V., Offermanns, S., and Simon, M. I. (2002) Interaction of $G\alpha_{12}$ with $G\alpha_{13}$ and $G\alpha_q$ signaling pathways. *Proc. Natl. Acad. Sci. U.S.A.* **99,** 9352–9357
36. Swiercz, J. M., Worzfeld, T., and Offermanns, S. (2009) Semaphorin 4D signaling requires the recruitment of phospholipase Cγ into the plexin-B1 receptor complex. *Mol. Cell. Biol.* **29,** 6321–6334
37. Oinuma, I., Katoh, H., Harada, A., and Negishi, M. (2003) Direct interaction of Rnd1 with Plexin-B1 regulates PDZ-RhoGEF-mediated Rho activation by Plexin-B1 and induces cell contraction in COS-7 cells. *J. Biol. Chem.* **278,** 25671–25677
38. Ohtsu, H., Mifune, M., Frank, G. D., Saito, S., Inagami, T., Kim-Mitsuyama, S., Takuwa, Y., Sasaki, T., Rothstein, J. D., Suzuki, H., Nakashima, H., Woolfolk, E. A., Motley, E. D., and Eguchi, S. (2005) Signal-crosstalk between Rho/ROCK and c-Jun NH_2-terminal kinase mediates migration of vascular smooth muscle cells stimulated by angiotensin II. *Arterioscler. Thromb. Vasc. Biol.* **25,** 1831–1836
39. Ying, Z., Jin, L., Palmer, T., and Webb, R. C. (2006) Angiotensin II upregulates the leukemia-associated Rho guanine nucleotide exchange factor (RhoGEF), a regulator of G protein signaling domain-containing RhoGEF, in vascular smooth muscle cells. *Mol. Pharmacol.* **69,** 932–940
40. Panizzi, J. R., Jessen, J. R., Drummond, I. A., and Solnica-Krezel, L. (2007) New functions for a vertebrate Rho guanine nucleotide exchange factor in ciliated epithelia. *Development* **134,** 921–931
41. Nishimura, T., Honda, H., and Takeichi, M. (2012) Planar cell polarity links axes of spatial dynamics in neural-tube closure. *Cell* **149,** 1084–1097
42. Kelly, P., Casey, P. J., and Meigs, T. E. (2007) Biologic functions of the G_{12} subfamily of heterotrimeric g proteins. Growth, migration, and metastasis. *Biochemistry* **46,** 6677–6687
43. Kuner, R., Swiercz, J. M., Zywietz, A., Tappe, A., and Offermanns, S. (2002) Characterization of the expression of PDZ-RhoGEF, LARG and $G\alpha_{12}$/$G\alpha_{13}$ proteins in the murine nervous system. *Eur. J. Neurosci.* **16,** 2333–2341